33rd Annual International Conference of the IEEE EMBS
Boston, Massachusetts USA, August 30 - September 3, 2011

Recovery of neural activity from nerve cuff electrodes

B Wodlinger *Student Member, IEEE* and DM Durand, *Fellow IEEE*

***Abstract*—The ability to recover signals from the peripheral nerves would provide natural and physiological signals for controlling artificial limbs and neural prosthetic devices. Current cuff electrode systems can provide multiple channels but the signals have low signal to noise ratio and are difficult to recover. Previous work has shown that beamforming algorithms provide a method to extract such signals from peripheral nerve activiy [1]. This paper describes in-silico and in vivo experiments done to validate that method in a more realistic case. A modified beam forming algorithm capable of significantly decrease cross talk between channels is described and the results of the a 16-channel Flat Interface Nerve Electrode used to recover signals from the sciatic nerve in rabbit while the distal tibial and peroneal branches were stimulated The beamforming spatial filters were able to distinguish which branch was being stimulated, and in many cases how strongly, over a large range of stimulation intensities.**

INTRODUCTION

Recording from peripheral nerves presents the opportunity not only to recover the signals of a wide variety of physiological sensors, but also physiological command signals controlling the functions of muscles and other organs. Even though this technology presents a variety of opportunities, it also presents several challenges. Attempts to address the mixing of biological signals have been made for a number of approaches. Classifiers have shown interesting results at decoding hand movements, and spatial filters have also been recently applied to this problem. Tesfayesus and Durand [3] recently applied blind source separation to perform similar de-mixing of the recorded signals, without the need for a model of the nerve geometry. These techniques will be discussed below with particular emphasis to those presented in Wodlinger and Durand [1] as they been have investigated thoroughly in both simulation and animal models.

Signal separation algorithms fall into three main categories: Inverse Problems (IP), Blind Source Separation (BSS) and Beamforming/Spatial Filtering (BF). These techniques are each reviewed below.

1. Inverse problem solutions (IP)

Inverse problem algorithms are based on the idea that a rigorous and complete forward model of the system can be found. This model can then be inverted so that for a given output one can calculate a (usually infinite) set of likely inputs. [4]. However, as a matrix inversion is required, the results can be slow and sensitive to model inaccuracy or choice of regularization parameter.

Manuscript received April 15, 2011. Financial support was provided by NIH grant 5R01NS032845-11 to DM Durand.
B. Wodlinger is currently in the Dept. of Physical Medicine & Rehabilitation University of Pittsburgh, Pittsburgh, PA
D.M. Durand is with Case Western Reserve University, Neural Engineering Center, Cleveland OH 44118 USA

2. Blind source separation

Blind source separation uses statistical information in the recordings to automatically de-mix the neural signals. This technique makes two important assumptions; the first is that the neural signals are only mixed linearly, an assumption supported by Maxwell's equations of the quasi-static propagation of current in the volume conductor. The second assumption is that the neural signals are statistically independent, such that maximizing the statistical independence of linear combinations of the recordings can reproduce them. This assumption is less clear and may depend on the nature of the training data available and the relationship between the signals of interest.

BSS algorithms also introduce a permutation ambiguity, where sources can appear swapped between successive time windows. This ambiguity can be readily solved using techniques presented in [3], who demonstrate the benefits of BSS techniques to nerve cuff recordings.

3. Spatial Filtering or Beamforming

Spatial filtering, or Beamforming, presents a compromise between techniques requiring extensive accurate models and those requiring none. Rather than trying to explicitly invert the given model, these techniques calculate a set of (usually linear) filters which can be applied to new data to estimate source levels. Spatial filtering methods are particularly well suited to nerve cuffs because of the spatial separation between functional (fascicular) sources, and small internal area of the cuff.

Filters can be calculated using a number of methods, from simple Laplacian operators used to take the second spatial difference to methods requiring the sensitivity fields of each contact on the electrode. These techniques are generally very fast after training, requiring a simple matrix multiplication at each time step. However they suffer from poor performance compared to IP algorithms, and so they are often combined with a post-processing stage to improve performance. This post-processing is usually adaptive in nature, for example the large array of techniques presented in [5].

A variation of a beamforming technique is presented in the following sections, and in more details in [6]. This beamforming filter is calculated using an FEM model of the nerve cuff in saline, and includes a static (i.e. non-adaptive) post-processing technique to improve separation quality without requiring statistical independence of the signals. Results are presented to demonstrate the performance of the system on simulated and animal model data.

METHODS

Beamforming Algorithm mapping

A computer model of a flat interface peripheral nerve electrode (FINE) placed on a homogenous nerve model is modeled (Fig. 1). This Finite Element Model (FEM) may be used to calculate the lead-field matrix, or forward problem, which relates the voltage recorded on each contact to the source current at each voxel within the nerve.

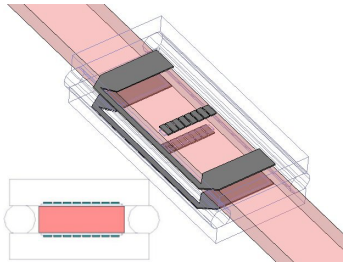

Fig. 1. The model used to generate the Transformation Matrix. The cuff has a 5mm x 1.5mm lumen and 8 recording contacts per side. Recording is performed using a quasi-tripolar technique by referencing the large outer electrodes at the openings of the cuff. Note that this model includes no nerve geometry, and so can be solved before cuff implantation. The cuff is made of silicone and enclosed in a large saline bath.

To calculate the Beamforming Filter Matrix, the weights (t_i) on the sensitivity vectors (S) for each contact are optimized for a source signal located in a single ideal pixel (δ_i). The following equation (1) is solved for each pixel i where,

$$St_i = \delta_i \quad (1)$$

Assuming n recording contacts and m pixels in the desired reconstruction, the variables are $S^{\{mxn\}}$, the sensitivity matrix, and $t_i^{\{nx1\}}$ the linear coefficients of the Beamforming Filter Matrix. Note that this equation is entirely independent of time and considers only the static behavior of the model. For increased efficiency, the reduced QR factorization of $S^{\{mxn\}}$ is first calculated so that for δ_i equal to the delta function at index i, the solution reduces to Equation 2, below, where q^*_i is the ith row of Q (since Q is orthogonal, the transpose acts as an inverse on the range). Normalization is performed for each set of weights, as in Equation 3.

$$t_i = R \setminus q_i^* \quad (2)$$

$$t_i = \frac{t_i}{\|St_i\|} \quad (3)$$

The column vectors t_i can then be concatenated to form the Beamforming filter matrix $T^{\{mxn\}}$, which operates on a single time point t of observed data ($o^{\{nx1\}}$) to produce the estimated activity at each pixel ($\hat{a}^{\{mx1\}}$) at time t , as in Equation 4. This activity vector can then be displayed as an image of the estimated activity in the plane of interest. Repeated application of the Beamforming filter matrix at different time points gives the time dependence to this procedure.

$$\hat{a} = To \quad (4)$$

When the Beamforming filter matrix is multiplied by the vector of voltages on each contact (Equation 4), an image is created providing an estimate of the activation of each pixel within the cross-section of nerve. A simple local-maxima-based algorithm was used to locate sources in the estimate using automatic thresholding to remove areas of low activity [7]. Morphological opening (erosion followed by dilation) which removes islands and peninsulas below a given size from a binary image was applied to prevent the algorithm from finding small sources near the periphery associated with noise. Once the fascicle locations are determined, the beamformers for those locations are applied to the full time-signal in order to reconstruct the fascicular activity. Post-processing techniques, such as RMS windowed averaging or BSS, can improve SNR and reduce cross-talk.

Filters for a given real neural source may be calculated by averaging the columns of T over which activity is observed. To improve the determination of the spatial extent of the sources, new filters are generated to take into account information from other locations. The filters from each pixel are weighted by the value of the source image at that pixel and averaged. This method places more emphasis on locations where the source is stronger, and provides some spatial averaging to reduce noise.

$$f_i = S_i^T M \quad (5)$$

Where n is the number of contacts, m is the number of pixels, $f_i^{\{1 \times n\}}$ is the filter for the i^{th} source, $S_i^{\{m \times 1\}}$ is the source image for that source, and $M^{\{m \times n\}}$ is the Beamforming Filter Matrix. In order to reduce sensitivity to areas with high interference, the spatial locations causing interference are iteratively subtracted from each filter using the following:

1. Calculate the interference (I_{ij}) due to source j picked up by the filter for source i
   $$I_{ij} = (Mf_i^T)^T S_j \mid i \neq j \quad (6)$$
2. Subtract or add the difference between the images, multiplied by the amount of incorrect signal in each to reduce the amount of interfering signal
   $$S_i = S_i - \sum_{(j|j\neq i)} I_{ij}(S_j - S_i) \quad (7)$$
3. Repeat, also recalculating the filters as in equation 7, until: threshold reached, or previous iteration was ineffective at removing inference

Experimental Methods:

New Zealand White Rabbits were used for this study. Anesthesia was induced with ketamine/diazepam and maintained with alpha-chloralose and buprenex. All protocols were approved by the Case Western Reserve University IACUC. Recordings were made from a novel 16-channel tripolar Flat Interface Nerve Electrode (FINE) placed on the sciatic trunk near the popliteal fossa, and amplified by an RHA1016 preamplifer chip (Intan Technologies, Utah) with low-pass filter set at 5kHz before undergoing A-to-D conversion and sampling at 15 kHz/channel. Tripolar stimulating FINE cuffs were placed on the Tibial and Peroneal branches of the Sciatic, distal to the recording cuff. Stimulation was applied to one of these cuffs at a time using 130Hz, 5kHz, or 10kHz sinusoids. Signals were post-processed using an 800Hz high-pass filter to ensure removal of any remaining EMG artifacts. A schematic of the setup is shown in Fig. 2. These stimulation paradigms allow both large CAP-like activity and lower-SNR pseudospontaneous activity to be collected and used for three offline experiments.

RESULTS

Signal Recovery in computer models

To form an accurate model of recorded neural activity a volume conductor FEM was combined with template models of action potentials as in [8-9]; [10]. These templates are randomly delayed and summed to create a simulated ENG signal with the desired temporal characteristics.

In order to examine the localization capability of the beamforming filters,

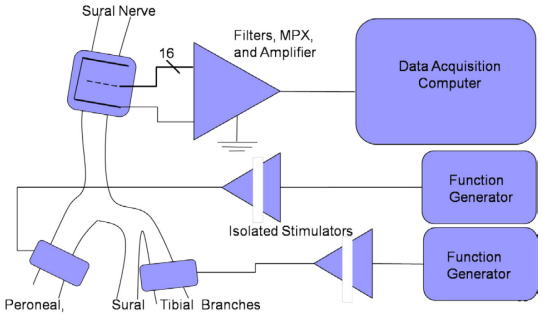

Fig. 2. Schematic of the experimental setup. A 16-channel quasi-tripolar FINE is placed on the main sciatic trunk, and two tripolar stimulating FINE are placed on the peroneal and tibial branches, distally. Stimulation is provided through isolated voltage-to-current stimulators and recorded using an Intan Tech. RHA1016 preamplifier.

a simulated signal isolated to a particular fascicle was created as described above (Figure 4a). The signal power (RMS) at each contact was calculated in 10 ms bins, and the beamforming localization procedure was applied to each one (Figure 3b) and the mean of the resulting list of sources calculated. This estimated location (green cross, Figure 3c) was then compared to the known location (red square, Figure 3c) and overlaid onto the fascicle map of the nerve for reference. This process was repeated and the results for one trial of all 10 fascicles at 40% noise are shown in Figure 3d, where the estimated source is shown as a green circle and the true location a red square. Even at this noise level, the figure clearly shows that all 10 sources are located to within their respective fascicles.

In noise-free signals, sources could be located to within 0.14±0.03 mm (N=100) of their fascicle's center. As the noise level was increased to 40%, the mean and standard deviation both increase to 0.18±0.17 mm (N=100). These results suggest that the location of single sources can be identified to 180±170 µm even in the presence of significant noise in the signal.

In a physiological situation, there would likely be more than two fascicles from which to record (depending on the nerve and location). Therefore, we tested the ability of the algorithm to recover signals from *n* simultaneously active fascicles, for *n* from 1 to 10, assuming the true source locations were known. For up to 5 simultaneously active fascicles, the reconstruction accuracy is unchanged with a mean value of R=0.74±0.18 (N=50). The accuracy decreases steadily as the number of active fascicles grows larger than 5, reaching 80% of the single fascicle value for 10 simultaneously active fascicles. Recording noise has a strong effect on the reconstruction, lowering the mean value of the *n*=1…5 trials to R=0.61±0.18 (N=50), and dropping to 65% of the noisy single fascicle value for 10 simultaneously active fascicles.

Signal Recovery in rabbit sciatic nerves.

The beamforming algorithm with Source-Based Filter post-processing is demonstrated in a Rabbit sciatic nerve model. The high-density FINE was placed on the main trunk of the sciatic nerve near the popliteal fossa, while smaller

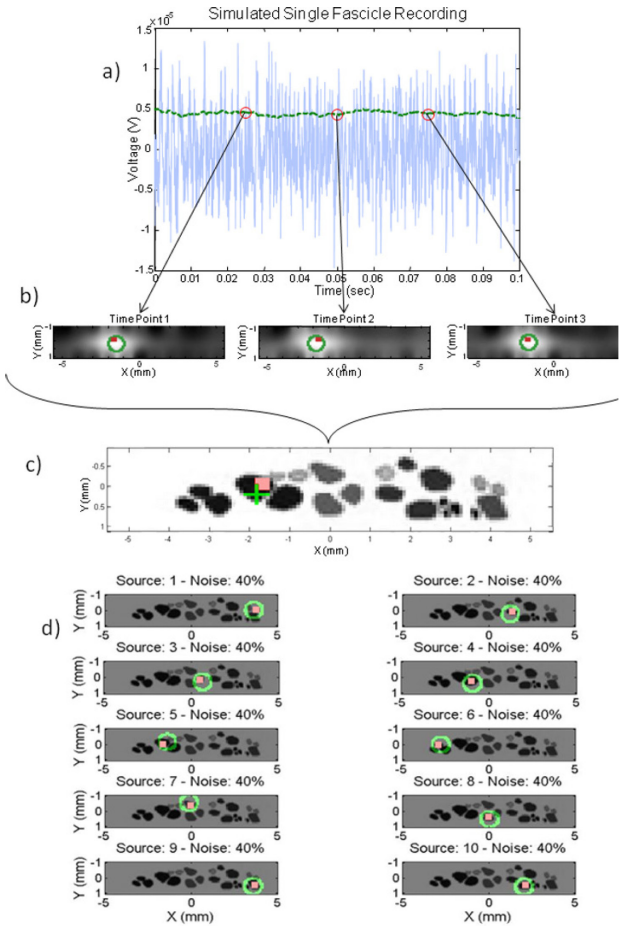

Figure 3. Localization Using Realistic Signals. a) Sample signal of single fascicle activity recorded on a single contact. The signal power (RMS) is shown as a dark thick line, while the raw signal is light and thin. b) Localization results for each of the 3 marked timepoints in (a). The estimated location is marked with a green circle, and the actual location with a red square. c) To locate the source, the mean location of all reconstructions is used. This final localization result is shown superimposed on the fascicle map, with the estimate marked by a cross and the true location by a square. d) Localization results for all fascicles (single trial at 40% noise). The fascicle map is shown in grey, with true source locations as red squares, and a green circle centered on the estimated location. 10 trials, each 100ms, were performed for each of the 10 fascicles modeled. The accuracy for the 40% noise trials, as pictured here, was 0.18±0.17 mm (N=100). Figure reproduced from [1] with permission from IEEE-TNSRE.

stimulating cuff electrodes were placed on the two main branches, the tibial and peroneal. These smaller cuffs were stimulated with pulses to elicit compound action potentials which could be used to localize the activity from the two fascicle groups originating in the two branches. Sinusoidal stimulation was also delivered to create more realistic patterns of activity. This sinusoidal stimulation has the added benefit that any stimulation artifact can be easily removed from the recordings using filtering. This is not the case for traditional pulse stimulation due to the large number of harmonics created. Low-frequency sinusoids were found to elicit CAP-like discharges in phase with the sinusoid, while high-frequency stimulation produced pseudo-random activity, as described in [11].

High frequency sinusoids were used to elicit pseudo-random activity in both fascicle groups in overlapping time windows. This test was repeated on 5 separate nerves and one typical example is shown in Figure 4. The upper frame

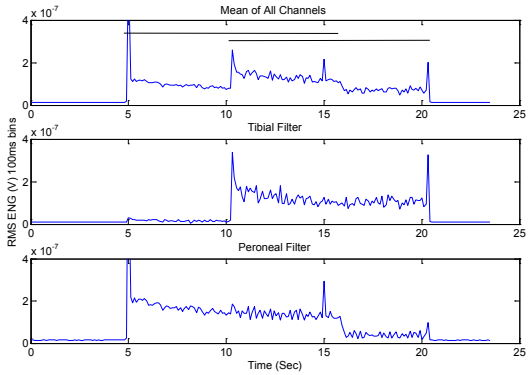

Figure 4. Overlapping stimulation of the Peroneal and Tibial branches. (Top) The mean of all 16 channels in the rectified, integrated recording. Black bars indicate stimulation periods for the Peroneal (left) and Tibial (right) branches. (Middle) Output after applying Tibial beamforming filter to the rectified, integrated signal. (Bottom) Output after applying Peroneal beamforming filter to the rectified, integrated signal. The cross talk between the two branches was 23±13% (n=10).

shows the mean of all 16 channels in the rectified and 100ms bin-integrated recording. The mean of the 16 channels is used for clarity, since the 16 raw channels are difficult to visualize. The lower two frames show the outputs of the beamforming filter matrix with SBF post-processing acting on the rectified, 100 ms bin-integrated recording. The black bars in the upper frame correspond to the stimulation intervals, with the Peroneal branch stimulated first. The cross-talk between the two branches was 23±13%, calculated using periods when only one of the two branches was active, on 10 signals from 5 nerves. Without a reference for comparison uncontaminated by the overlapping activity the accuracy of the separation cannot be calculated outside the windows where only one source was active.

DISCUSSION

Many techniques have been proposed to separate individual fascicular signals from whole peripheral nerve recordings, including Inverse Problem techniques, Blind Source Separation, and Beamforming. While Inverse Problem techniques rely heavily on the accuracy of the system model, Blind source techniques do not assume any particular model, requiring only linear mixing of the statistically independent source signals. Beamforming represents a compromise, making use of some of the available model. A beamforming algorithm was investigated, along with a Source-based Filter post-processing, on both artificial and real neural recordings and demonstrated to provide R^2=0.81±0.08 separation of signals from 2 independent fascicular groups.

The ability to recover neural signals is only the first step in the larger goal of a closed loop system for neural control. A major component is the ability to control neural function with multiple contact nerve peripheral nerve electrodes. The following section describes in-silico and in-vivo experiments to study the ability of the FINE cuff to control the ankle joint.

ACKNOWLEDGMENT

The project described was supported by Grant Number R01 NS032845-10 from the National Institutes of Health (NINDS). The content is solely the responsibility of the authors and does not necessarily represent the official views of the National Institutes of Health.

REFERENCES

[1] B. Wodlinger and D. M. Durand, "Localization and Recovery of Peripheral Neural Sources With Beamforming Algorithms," *Ieee Transactions on Neural Systems and Rehabilitation Engineering,* vol. 17, pp. 461-468, Oct 2009.

[2] P. M. Rossini, *et al.*, "Double nerve intraneural interface implant on a human amputee for robotic hand control," *Clin Neurophysiol,* vol. 121, pp. 777-83, May 2010.

[3] W. Tesfayesus and D. M. Durand, "Blind source separation of peripheral nerve recordings," *J Neural Eng,* vol. 4, pp. S157-67, Sep 2007.

[4] A. Nissinen, *et al.*, "The Bayesian approximation error approach for electrical impedance tomography - experimental results," *Measurement Science & Technology,* vol. 19, pp. -, Jan 2008.

[5] K. Sekihara and S. S. Nagarajan, *Adaptive Spatial Filters for Electromagnetic Brain Imaging*: Springer, 2008.

[6] B. Wodlinger and D. M. Durand, "Peripheral nerve signal recording and processing for artificial limb control," *Conf Proc IEEE Eng Med Biol Soc,* vol. 2010, pp. 6206-9, 2010.

[7] N. Otsu, "A Threshold Selection Method from Gray-Level Histograms," *IEEE Transactions on Systems, Man, and Cybernetics,* vol. 9, pp. 62-66, 1979.

[8] S. Jezernik and T. Sinkjaer, "On statistical properties of whole nerve cuff recordings," *IEEE Trans Biomed Eng,* vol. 46, pp. 1240-5, Oct 1999.

[9] P. B. Yoo and D. M. Durand, "Selective recording of the canine hypoglossal nerve using a multicontact flat interface nerve electrode," *IEEE Trans Biomed Eng,* vol. 52, pp. 1461-9, Aug 2005.

[10] W. Tesfayesus, P. Yoo, M. Moffitt, and D. M. Durand, "Blind Source Separation of Nerve Cuff Recordings," in *Proceedings of the 25th International Conference of the IEEE/EMBS*, Cancun, Mexico, 2003.

[11] J. T. Rubinstein, *et al.*, "Pseudospontaneous activity: stochastic independence of auditory nerve fibers with electrical stimulation," *Hear Res,* vol. 127, pp. 108-18, Jan 1999.